



Triangular DNA Origami Tilings

Grigory Tikhomirov,^{†,§} Philip Petersen,^{‡,§} and Lulu Qian^{*,†,§}

[†]Bioengineering, California Institute of Technology, Pasadena, California 91125, United States

[‡]Biology, California Institute of Technology, Pasadena, California 91125, United States

[§]Computer Science, California Institute of Technology, Pasadena, California 91125, United States

Supporting Information

ABSTRACT: DNA origami tilings provide methods for creating complex molecular patterns and shapes using flat DNA origami structures as building blocks. Square tiles have been developed to construct micrometer-scale arrays and to generate patterns using stochastic or deterministic strategies. Here we show triangular tiles as a complementary approach for enriching the design space of DNA tilings and for extending the shape of the self-assembled arrays from 2D to 3D. We introduce a computational approach for maximizing binding specificity in a fully symmetric tile design, with which we construct a 20-tile structure resembling a rhombic triacontahedron. We demonstrate controlled transition between 3D and 2D structures using simple methods including tile concentration, magnesium, and fold symmetry in tile edge design. Using these approaches, we construct 2D arrays with unbounded and designed sizes. The programmability of the edge design and the flexibility of the structure make the triangular DNA origami tile an ideal building block for complex self-assembly and reconfiguration in artificial molecular machines and fabricated nanodevices.

The invention of DNA origami¹ has deepened the understanding of how molecules could interact with each other in a complex self-assembly process and has accelerated the engineering of molecular systems with custom-designed structures and programmable behaviors. Using DNA origami structures as tiles to create two-dimensional arrays, in solution^{2–6} or on a surface,^{7–9} has enabled precise organization of nanoparticles^{10,11} for fabricating larger nanodevices and has opened up the possibility for building spatially organized DNA circuits¹² on larger breadboards and prototyping molecular robots^{13–16} on larger testing grounds.

In prior work, we designed a square DNA origami tile for creating unbounded arrays with combinatorial patterns that have random-yet-controlled properties¹⁷ and arrays of designed sizes with arbitrary patterning capability.¹⁸ However, the square is only one of three regular polygons with the two-dimensional (2D) space filling property, and the shapes and patterns that can be created with a combination of squares and triangles become much more interesting than squares alone.¹⁹ Here we aim to understand (i) if the design principles for creating square tiles can be generalized to triangular tiles, (ii) if new design principles are needed for programming the

interactions between tiles, considering the difference in geometry, and (iii) if the transition between 2D and 3D structures can be controlled in triangular origami tilings, especially using simple methods that do not require major changes in the tile design.

Similar to the square tile design, we chose a scaffold path for the triangle shape that is rotationally symmetric with maximally continuous surface area (Figures 1a and S1). A set of 16 edge

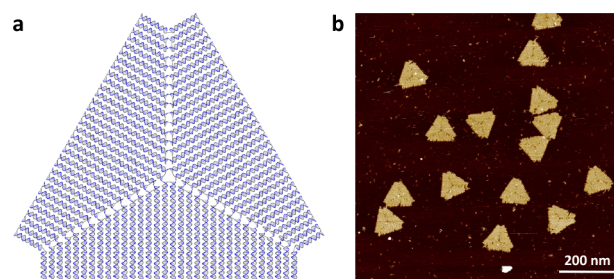


Figure 1. A triangular DNA origami tile. (a) Design of an equilateral triangle composed of three isosceles triangles. A 3D model is described in [Supplementary Note S2](#) and Cadnano²⁰ diagram shown in [Figure S9](#). (b) AFM image of the triangular DNA origami tiles as monomers.

staples on each side of the equilateral triangle can be modified to provide weak tile–tile interactions using stacking bonds and short sticky ends. Atomic force microscopy (AFM) images showed that the triangular origami tile was well formed with an estimated yield of 92.3% (Figures 1b and S2).

We have previously learned that stacking bonds alone could not provide sufficient specificity for the self-assembly of large, 2D arrays, and short sticky ends are desired for introducing additional specificity while still keeping the tile–tile interactions weak enough for avoiding kinetic traps during self-assembly.¹⁷ One property of the previous design is that the sequences of the sticky ends depend on the sequence of the M13 scaffold, naturally allowing unique edge interactions. However, it also resulted in a limitation that a truly symmetric tile with identical sticky end sequences on all edges could not be created.

Here we explore a new design principle that involves a computational search for maximizing common sticky end sequences on all tile edges. Because M13 is a circular strand,

Received: October 5, 2018

Published: December 4, 2018



any nucleotide location can be used as a starting point of the scaffold for designing staple strands. We computed the total number of common nucleotides at the 5' and 3' ends of the three staples at each of the 16 locations along the three edges of the triangular tile for all possible starting points of the scaffold. Among the starting points with largest number of common nucleotides, we chose one with good sequence diversity and balanced nucleotide locations. Using these nucleotides as sticky ends, a fully symmetric tile was then created, in which each edge is complementary to itself as well as to the other two edges (left diagram in Figure 2a). A total of

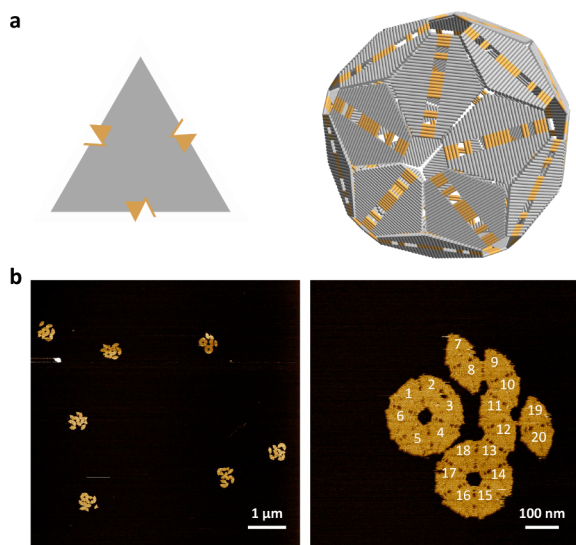


Figure 2. A 20-tile structure interpreted as a rhombic triacontahedron. (a) Abstract design diagram of a symmetric tile (left) and interpretation of the self-assembled structure (right). Solid arrow facing outward combined with hollow arrow facing inward indicates a self-complementary edge that has both extended and truncated staples. Detailed edge design is shown in Figure S7. (b) AFM images. Despite that hexagon shapes do not appear in the 3D structure, they were observed in some flattened 2D structures, presumably because recombination of triangular tiles could take place on a mica surface.

12 1-nt sticky ends and 8 stacking bonds were employed on each edge, which is stronger than the previously developed square tiles.¹⁷ Note that the tile design is still compatible with creating unique edge interactions, as different choices of staple truncations and extensions can be made.

With the symmetric triangular tile, we attempted constructing unbounded arrays. To our surprise, the structures observed in AFM images were small groups of triangles, some of which were not even connected (Figure 2b). Furthermore, the number of triangles in each group was consistently 20 (Figure S3a). We hypothesized that instead of forming 2D arrays, the tiles self-assembled into a closed 3D structure; during AFM imaging, because of the attraction to the flat mica surface, each 3D structure opened up along random edges, resulting in a variety of relative positions between tiles but all tiles in the same 3D structure remained close to each other. Transmission electron microscopy (TEM) images showed spherical structures with an estimated diameter of 205.4 ± 11.1 nm (Figure S3b), agreeing with the diameter of an inscribed sphere of an icosahedron made of 20 equilateral triangles (i.e., approximately 205 nm).

Forming an icosahedron requires the tiles to bend at a small angle along the edges, which is incompatible with the orientation of the stacking bonds, and the tile–tile interactions would have to rely on sticky ends only. However, forming a rhombic triacontahedron simply requires the tiles to bend at an even smaller angle along the seams between the three isosceles triangles, which is presumably easier because of the flexibility of the single-stranded domains in the bridge staples (right diagram in Figure 2a). In fact, a tile that has just stacking bonds was also able to form 20-tile structures in AFM images (Figure S4), indicating that the 3D structure is more likely to be a rhombic triacontahedron.

This unexpected result led us to investigate how to control the transition between 2D and 3D structures using the same tile design. We found that the symmetric triangular tile self-assembled into rhombic triacontahedra at lower tile concentration with more magnesium but into unbounded 2D arrays at higher tile concentration with less magnesium (Figure S3c). It is known that if there are multiple possible reaction pathways requiring different numbers of reactants, lower order reactions are preferred when the reactants are at a sufficiently low concentration. Because closing up a 3D structure requires unimolecular reactions while growing a 2D array requires bimolecular reactions, it is reasonable to assume that the 3D structure is preferred at lower concentrations. It is also known that magnesium stabilizes DNA hybridization²¹ and reduces interhelical spacing in DNA origami.²² Less magnesium would result in a lower melting temperature of the arrays, which means the tiles are presumably more rigid when self-assembling into arrays at a lower temperature and thus bending within the structure would be discouraged. Meanwhile, slight expansion of the origami structure may have altered the possible intrinsic curvature of the tiles, favoring the formation of 2D arrays.

Alternatively, changing the tile design to be asymmetric could also encourage the formation of 2D arrays (Figure 3a). In this design, one tile edge is self-complementary (colored in

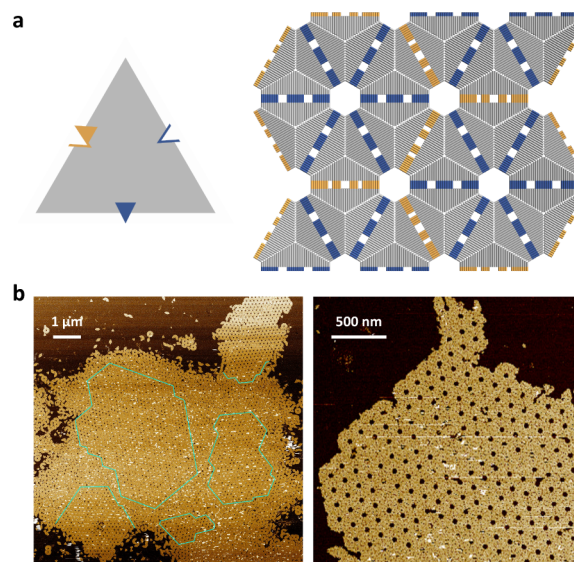


Figure 3. Unbounded 2D array. (a) Abstract design diagram of an asymmetric tile (left) and interpretation of the self-assembled structure (right). Detailed edge design is shown in Figure S7. (b) AFM images. The boundaries of crystalline areas are highlighted in cyan.

orange) while the two other edges are complementary to each other (colored in blue). Because the sticky end sequences are no longer common, the result of the computational search no longer plays a role here, but the locations of the edge staples were chosen to allow 6 G/C and 6 A/T base pairs on both orange and blue edges to roughly balance the strength of binding. There are two alternating configurations of a hexagon-shaped six-tile neighborhood in a 2D array: one with six blue edges and the other with three blue and three orange edges. If the 2D array with some missing tiles were to fold up into a 3D structure, it would be possible to create a vertex where five blue edges meet, but it would be impossible to have an odd number of edges meet at a vertex if they are blue and orange. Therefore, this asymmetric tile design is incompatible with the geometry of an icosahedron or rhombic triacontahedron. AFM images showed 2D arrays with crystalline areas of up to approximately $3.5 \times 4.5 \mu\text{m}$ (Figure 3b).

Replacing the self-complementary edge in the asymmetric tile with an inert edge allows the self-assembly of structures with designed sizes (Figure 4a). Similar to how rhombic

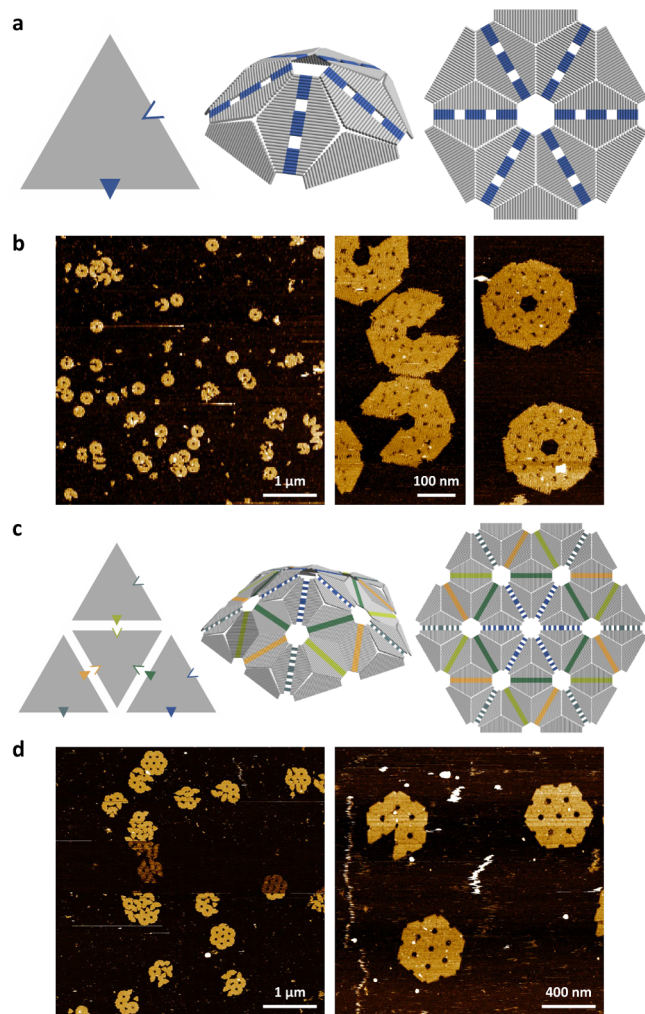


Figure 4. Structures with designed sizes in mixtures of 2D and 3D. (a) Abstract design diagrams and (b) AFM images of small hexagons mixed together with a 5-tile pacman-like structure. (c) Abstract design diagrams and (d) AFM images of large hexagons mixed together with a 20-tile pacman-like structure. Detailed edge design is shown in Figure S7.

triacontahedra were formed, in addition to a hexagon shape, this tile is also capable of forming a 3D dome structure. Indeed, both hexagons and 5-tile structures were found in the AFM images, severely limiting the yield of hexagons (Figure 4b). The same phenomenon occurred with four unique tiles designed to form a larger hexagon (Figure 4cd).

The same principle of how the asymmetric tile design discouraged the formation of 3D structures can be applied to structures with designed sizes. For example, two unique tiles can be used to create a small hexagon (Figure 5a). Using two

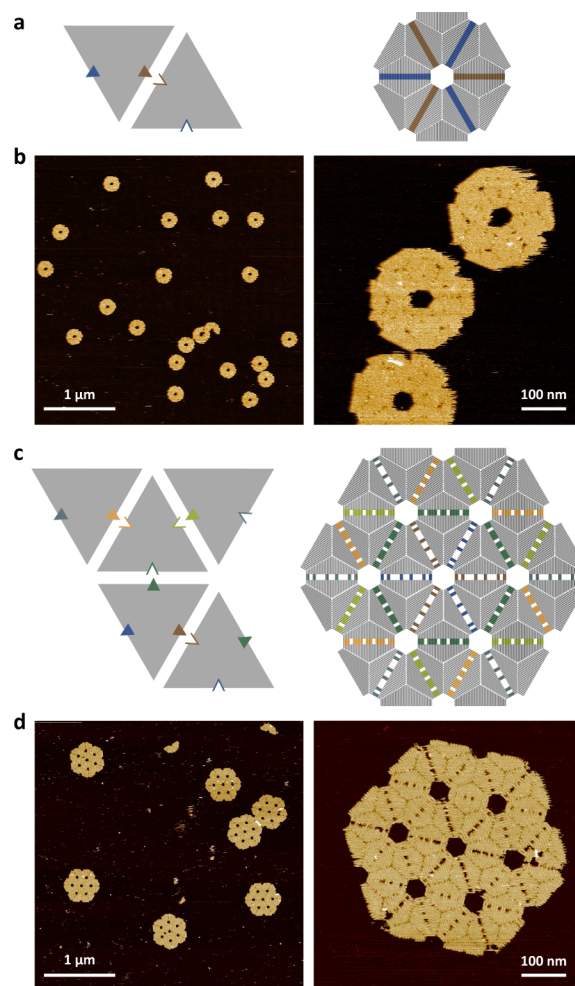


Figure 5. 2D arrays with designed sizes. (a) Abstract design diagrams and (b) AFM images of small hexagons. (c) Abstract design diagrams and (d) AFM images of large hexagons. Detailed edge design is shown in Figure S8.

alternating edges, structures with an even but not odd number of tiles are possible. AFM images showed well-formed hexagons with a diagonal of approximately 270 nm (Figure 5b) and the yield was estimated to be 75.1% (Figure S5).

Similarly, a larger hexagon can be created using five unique tiles (Figure 5c). Compared to the design shown in Figure 4c, one additional tile was used to create two alternating edges within the small hexagon shape at the center of the large hexagon. To encourage a one-pot two-staged self-assembly process, stronger (and weaker) edge interactions with 12 (and 6) staples were used among the four tiles forming a larger triangle (and six larger triangles forming a hexagon). As shown in the AFM images (Figure 5d), hexagons with a diagonal of

approximately 540 nm were constructed with an estimated yield of 35.4% (Figure S6).

We have shown that a triangular DNA origami tile can be created to self-assemble into 2D and 3D structures with unbounded and designed sizes. Unlike the previously developed triangular DNA origami structure,^{1,8,9} this new tile has DNA helices arranged perpendicular to all three edges, which enabled a high level of programmability for creating edge interactions with desired specificity and binding energy, utilizing a combination of stacking bonds and short sticky ends. Importantly, the structural flexibility of the tile, especially the possibility to bend along the seams between adjacent isosceles triangles composing the equilateral triangle, allows for the formation of 3D structures. If desired, specific degree of bending could potentially be induced by programming the lengths of single-stranded domains²³ in bridge staples. The same kind of structural flexibility also plays an important role in programming the dynamic interactions between DNA origami structures, through a mechanism that we termed tile displacement.²⁴ Combining the triangular tile with the previously developed square tile will open up new opportunities for programming complex self-assembly and reconfiguration in molecular systems.

■ ASSOCIATED CONTENT

● Supporting Information

The Supporting Information is available free of charge on the ACS Publications website at DOI: 10.1021/jacs.8b10609.

Supporting methods, figures, and DNA sequences (PDF)

■ AUTHOR INFORMATION

Corresponding Author

*luluqian@caltech.edu

ORCID

Lulu Qian: 0000-0003-4115-2409

Author Contributions

[§]Equal contribution.

Notes

The authors declare no competing financial interest.

■ ACKNOWLEDGMENTS

The authors thank A. McDowall and A. Malyutin for the assistance with TEM imaging. G.T. and L.Q. were supported by a BWF grant (1010684) and the Shurl and Kay Curci Foundation. P.P. was supported by a NIH/NRSA training grant (5 T32 GM07616). L.Q. was also supported by an NSF award (1351081).

■ REFERENCES

- (1) Rothmund, P. W. K. Folding DNA to create nanoscale shapes and patterns. *Nature* **2006**, *440*, 297–302.
- (2) Liu, W.; Zhong, H.; Wang, R.; Seeman, N. C. Crystalline two-dimensional DNA-origami arrays. *Angew. Chem.* **2011**, *123*, 278–281.
- (3) Woo, S.; Rothmund, P. W. Programmable molecular recognition based on the geometry of DNA nanostructures. *Nat. Chem.* **2011**, *3*, 620–627.
- (4) Rajendran, A.; Endo, M.; Katsuda, Y.; Hidaka, K.; Sugiyama, H. Programmed two-dimensional self-assembly of multiple DNA origami jigsaw pieces. *ACS Nano* **2011**, *5*, 665–671.

- (5) Zhao, Z.; Liu, Y.; Yan, H. Organizing DNA origami tiles into larger structures using preformed scaffold frames. *Nano Lett.* **2011**, *11*, 2997–3002.
- (6) Zenk, J.; Tuntivate, C.; Schulman, R. Kinetics and thermodynamics of Watson-Crick base pairing driven DNA origami dimerization. *J. Am. Chem. Soc.* **2016**, *138*, 3346–3354.
- (7) Woo, S.; Rothmund, P. W. Self-assembly of two-dimensional DNA origami lattices using cation-controlled surface diffusion. *Nat. Commun.* **2014**, *5*, 4889.
- (8) Aghebat Rafat, A.; Pirzer, T.; Scheible, M. B.; Kostina, A.; Simmel, F. C. Surface-assisted large-scale ordering of DNA origami tiles. *Angew. Chem., Int. Ed.* **2014**, *53*, 7665–7668.
- (9) Suzuki, Y.; Endo, M.; Sugiyama, H. Lipid-bilayer-assisted two-dimensional self-assembly of DNA origami nanostructures. *Nat. Commun.* **2015**, *6*, 8052.
- (10) Wang, P.; Gaitanaros, S.; Lee, S.; Bathe, M.; Shih, W. M.; Ke, Y. Programming self-assembly of DNA origami honeycomb two-dimensional lattices and plasmonic metamaterials. *J. Am. Chem. Soc.* **2016**, *138*, 7733–7740.
- (11) Liu, W.; Halverson, J.; Tian, Y.; Tkachenko, A. V.; Gang, O. Self-organized architectures from assorted DNA-framed nanoparticles. *Nat. Chem.* **2016**, *8*, 867–873.
- (12) Chatterjee, G.; Dalchau, N.; Muscat, R. A.; Phillips, A.; Seelig, G. A spatially localized architecture for fast and modular DNA computing. *Nat. Nanotechnol.* **2017**, *12*, 920–927.
- (13) Lund, K.; Manzo, A. J.; Dabby, N.; Michelotti, N.; Johnson-Buck, A.; Nangreave, J.; Taylor, S.; Pei, R.; Stojanovic, M. N.; Walter, N. G.; Winfree, E.; Yan, H. Molecular robots guided by prescriptive landscapes. *Nature* **2010**, *465*, 206–210.
- (14) Gu, H.; Chao, J.; Xiao, S.-J.; Seeman, N. C. A proximity-based programmable DNA nanoscale assembly line. *Nature* **2010**, *465*, 202–205.
- (15) Wickham, S. F.; Endo, M.; Katsuda, Y.; Hidaka, K.; Bath, J.; Sugiyama, H.; Turberfield, A. J. Direct observation of stepwise movement of a synthetic molecular transporter. *Nat. Nanotechnol.* **2011**, *6*, 166–169.
- (16) Thubagere, A. J.; Li, W.; Johnson, R. F.; Chen, Z.; Doroudi, S.; Lee, Y. L.; Izatt, G.; Wittman, S.; Srinivas, N.; Woods, D.; Winfree, E.; Qian, L. A cargo-sorting DNA robot. *Science* **2017**, *357*, No. eaan6558.
- (17) Tikhomirov, G.; Petersen, P.; Qian, L. Programmable disorder in random DNA tilings. *Nat. Nanotechnol.* **2017**, *12*, 251–259.
- (18) Tikhomirov, G.; Petersen, P.; Qian, L. Fractal assembly of micrometre-scale DNA origami arrays with arbitrary patterns. *Nature* **2017**, *552*, 67–71.
- (19) Grünbaum, B.; Shephard, G. C. *Tilings and patterns*; Freeman, 1987.
- (20) Douglas, S. M.; Marblestone, A. H.; Teerapittayanon, S.; Vazquez, A.; Church, G. M.; Shih, W. M. Rapid prototyping of 3D DNA-origami shapes with caDNA. *Nucleic Acids Res.* **2009**, *37*, 5001–5006.
- (21) Owczarzy, R.; Moreira, B. G.; You, Y.; Behlke, M. A.; Walder, J. A. Predicting stability of DNA duplexes in solutions containing magnesium and monovalent cations. *Biochemistry* **2008**, *47*, 5336–5353.
- (22) Fischer, S.; Hartl, C.; Frank, K.; Radler, J. O.; Liedl, T.; Nickel, B. Shape and interhelical spacing of DNA origami nanostructures studied by small-angle X-ray scattering. *Nano Lett.* **2016**, *16*, 4282–4287.
- (23) He, Y.; Ye, T.; Su, M.; Zhang, C.; Ribbe, A. E.; Jiang, W.; Mao, C. Hierarchical self-assembly of DNA into symmetric supramolecular polyhedra. *Nature* **2008**, *452*, 198–201.
- (24) Petersen, P.; Tikhomirov, G.; Qian, L. Information-based autonomous reconfiguration in systems of interacting DNA nanostructures. *Nat. Commun.*, accepted. DOI: 10.1038/s41467-018-07805-7